Energy Reports 8 (2022) 6332–6346

Contents lists available at ScienceDirect

Energy Reports

journal homepage: www.elsevier.com/locate/egyr

Research paper

# Generalized regression neural network and fitness dependent optimization: Application to energy harvesting of centralized TEG systems

Adeel Feroz Mirza [a], Syed Kamran Haider [b], Abbas Ahmed [b], Ateeq Ur Rehman [c], Muhammad Shafiq [d,*], Mohit Bajaj [e], Hossam M. Zawbaa [f,g,*], Pawel Szczepankowski [a], Salah Kamel [h]

[a] Department of Power Electronics and Electrical Machines, Gdansk University of Technology, Poland
[b] Department of Electrical & Electronics Engineering, Beaconhouse International College, Islamabad 44000, Pakistan
[c] Department of Electrical Engineering, Government College University, Lahore 54000, Pakistan
[d] Department of Information and Communication Engineering, Yeungnam University, Gyeongsan 38541, Korea
[e] Department of Electrical and Electronics Engineering, National Institute of Technology Delhi, New Delhi 110040, India
[f] Faculty of Computers and Artificial Intelligence, Beni-Suef University, Beni-Suef, Egypt
[g] Technological University Dublin, Dublin, Ireland
[h] Electrical Engineering Department, Faculty of Engineering, Aswan University, 81542 Aswan, Egypt

ARTICLE INFO

*Article history:*
Received 7 February 2022
Received in revised form 8 April 2022
Accepted 3 May 2022
Available online xxxx

*Keywords:*
Thermoelectric generator (TEG)
Maximum power point tracking (MPPT)
Swarm intelligence (SI)
Relative error (RE)
Generalized regression neural network (GRNN)
Global maximum power points (GMPP)

ABSTRACT

The thermoelectric generator (TEG) system has attracted extensive attention because of its applications in centralized solar heat utilization and recoverable heat energy. The operating efficiency of the TEG system is highly affected by operating conditions. In a series-parallel structure, due to diverse temperature differences, the TEG modules show non-linear performance. Due to the non-uniform temperature distribution (NUTD) condition, several maximum power points (MPPs) appear on the P/V curve. In multiple MPPs, the true global maximum power points (GMPP) are very important for optimum action. The existing conventional technologies have slow tracking speed, low productivity, and unwanted fluctuations in voltage curves. To overcome the TEG system behavior and shortcomings, A novel control technology for the TEG system is proposed, which utilizes the improved generalized regression neural network and fitness dependent optimization (GRNNFDO) to track the GMPP under dynamic operating conditions. Conventional TEG system control techniques are not likely to trace true GMPP. Our novel GRNNFDO can trace the true GMPP for NUTD and under varying temperature conditions In this article, some major contributions in the area of the TEG systems are investigated by solving the issues such as NUTD global maxima tracking, low efficiency of TEG module due to mismatch, and oscillations around optimum point. The results of GRNNFDO are compared with the Cuckoo-search algorithm (CSA), and grasshopper optimization (GHO) algorithm and particle swarm optimization (PSO) algorithm. Results of GRNNFDO are verified with experiments and authenticated with MATLAB/SIMULINK. The proposed GRNNFDO control technique generates up to 7% more energy than PSO and 60% fast-tracking than meta-heuristic algorithms.



## 1. Introduction

Nowadays, the contribution of renewable sources is progressively increasing due to rising concern of $CO_2$ emission, better cost/watt promising governmental green energy-related policies, The most reviewed approaches to converting solar energy into electrical energy are PV systems, thermoelectric generation (TEG) systems, and concentrated PV-TEG (Mirza et al., 2021). The TEG systems were ignored due to the low power ratings, complex behavior under diverse temperatures, and implementation cost. Lately, the advanced engineering techniques, the finding of new materials, and revolutions in low-priced silicon manufacturing make TEG systems an ideal member of renewable energy sources (Mansoor et al., 2021).

* Corresponding authors.
*E-mail addresses:* adeel.mirza@pg.edu.pl (A.F. Mirza), kamran.haider@bic.edu.pk (S.K. Haider), abbas.ahmed@bic.edu.pk (A. Ahmed), ateeq.rehman@gcu.edu.pk (A.U. Rehman), shafiq@ynu.ac.kr (M. Shafiq), mohitbajaj@nitdelhi.ac.in (M. Bajaj), hossam.zawbaa@gmail.com (H.M. Zawbaa), pawel.szczepankowski@pg.edu.pl (P. Szczepankowski), skamel@aswu.edu.eg (S. Kamel).

https://doi.org/10.1016/j.egyr.2022.05.003

TEG module can endure high temperatures, so it is very suitable for solar energy applications. On the contrary, when the temperature is higher than room temperature, solar cells will lose efficiency (Garmejani and Hossainpour, 2021). Another advantage of TEG is that it can be connected in different configurations to get a high output power rating (Valera et al., 2021). DC converter also performs the control action of the reference voltage by modifying the duty cycle, which is defined as a control signal. This control action also allows the TEG system to work dynamically at max. attainable power. Fig. 1 displays the typical TEG system with an intelligent controller. The TEG module is connected to a centralized DC-DC boost converter that provides the interface between power and the load (Li et al., 2021). The duty cycle can be modified by PWM signal and MOSFET drive circuit provides control to achieve effective MPPT operation (Mohamed et al., 2021).

In the literature, numerous MPPT technologies are considered for renewable energy systems, including photovoltaic systems, wind power generation systems, and centralized TEG systems (Zafar et al., 2021). MPPT technologies can be separated into two categories: which are conventional technologies and intelligent technologies. Conventional MPPT methods are divided into analytical MPPT methods and gradient-based methods. Open-circuit voltage (OCV$V_{OC}$) based method, and short-circuit current (SCC $I_{SC}$) based MPPT method belong to analytical MPPT technologies. The disadvantage of these techniques is that the parameter values vary with the operating temperature. The issue with the TEG system is that parameters such as $V_{OC}$, $I_{SC}$ and efficiency is also dependent on working conditions. When the working conditions change, the operating efficiency will also be affected. Therefore, the setpoint needs to be adjusted regularly by removing the load. In addition, the main problems of these techniques are non-adjustable functioning, low efficiency, and the incapability to solve the NUTD problem. Various gradient-based MPPT algorithms for TEG systems have been established, which use a gradient-based procedure. Namely P&O (Ali and Mohamed, 2022), incremental conductance algorithm (ICA), and hill-climbing algorithm (HCA) (Ahmed and Salam, 2018).

The AI-based control technologies can be divided into FLC-based technologies, swarm intelligence (SI) based technologies, and Artificial Neural networks (ANN) based technologies (Sahri et al., 2021). The deep learning technologies use the ANN. ANN can efficiently handle the non-linear behavior, but a large number of training tests are required to train the system (Ali et al., 2021).

The multiple TEG modules can be organized in many configurations, such as series type configuration, parallel type configuration, or can be organized in series-parallel configuration (Yang et al., 2019). In the present work, a centralized TEG system with $DC-DC$ boost converter is used. Non-uniform temperature on TEG modules generates a mismatching current. As we know that current in a series circuit must be the same so to solve this issue a bypass diode can be connected in parallel combination with TEG modules (Kalyani et al., 2020; Khan et al., 2022). Bypass diode can be activated at different voltage magnitudes, which makes the non-linear behavior of TEG module even more complex. This problem is very prominent under NUTD conditions (Yedala and Kaisare, 2021). Hence, the centralized TEG system meaningfully reduces the DC-DC boost converter's costs. Centralized TEG system control can be regarded as an optimization problem. Compared with other technologies, the main advantage of most MPPT technologies based on swarm intelligence and an evolutionary algorithm is to track GMPP under NUTD. Heuristics algorithms such as cuckoo search algorithm(CSA) (Ahmed and Salam, 2014; Ma et al., 2013), particle swarm optimization (PSO) (Renaudineau et al., 2014; Ishaque et al., 2012; Priyadarshi et al., 2020), overall distribution (OD) algorithm (Li et al., 2018), grasshopper optimization (GHO) (Mansoor et al., 2020b), artificial bee colony (ABC) (soufyane Benyoucef et al., 2015), simulated annealing (SA) (Lyden and Haque, 2015), overall distribution (OD) algorithm (Li et al., 2018), Butterfly optimization algorithm(BOA) (Fathy, 2020), adaptive cuckoo optimization algorithm (ACOA) (Mirza et al., 2019), Harris hawk optimization (HHO) (Mansoor et al., 2020a), grey wolf optimization (GWO) (Mohanty et al., 2015; Darcy Gnana Jegha et al., 2020), salp swarm optimization algorithm (SSA) (Mirza et al., 2020), and particle swarm optimization gravitational search (PSOGS) have been studied. Performance of SI techniques is subjected to aspects such as initiated population size, information sharing mechanism between the swarms, total iterations, random parameters, and computational load (Zhao et al., 2020; Zafar et al., 2020).

The optimization techniques are based on randomly initialized populations and particles to search for the optimal location under different parameters. Fine-tuning of parameters and the initialization of the population can impact the performance of meta-heuristic based MPPT technologies (Li et al., 2018; Tariq et al., 2021). MPPT technology based on particle swarm optimization (PSO) uses the social interaction of swarm particles to share the information of the best global solution obtained by searching particles. In particle swarm position updating, the weighted vector influence is used to share the information. The scheme is helpful for the population to converge to the global best iterative solution. To break through local best iterative solution, arbitrary numbers are generated into the velocity $v_{pso}$ and position equations of PSO. The arbitrary number will produce unexpected oscillation and affect the stability time of the PSO algorithm (Huang et al., 2017). PSOGS combines the effective exploration of PSO through the precise development of GS, which greatly improves the work efficiency of PSO. Although the enhancement of steady-state oscillation can be observed, the stabilization time is not significantly minimized. The addition of GS into the PSO algorithm increases the quantity of constraints to be optimized, the technical difficulty and the computational power of system. ACO uses pheromones to communicate the information. Pheromones evaporate over time. Each ant is a member of a collection of possible solutions, so careful selection mechanisms are required. Scout ants are also used to explore search space (Priyadarshi et al., 2019). Due to the selection of candidate solutions and the probabilistic properties of their positions in the search space, an unexpected output will be produced. Similarly, in CSA, Levy flight is used to allocate random burst values, which will lead to undesirable fluctuations in the output signal (Ahmed and Salam, 2014). With the same inspiration, this paper proposes a novel hybrid technique. In which novel FDO is used to determine the spread parameter of GRNN to calculate the masses and biases values of hidden layer effectively. Novel GRNNFDO is tested under various operating conditions and concluded that it is very effective for tracking GMMP. The main contributions of this article are summarized as follows:

- The proposed learning-based GRNNFDO control technique requires less tracking time to trace the GMPP than other control techniques.
- GRNNFDO can trace the GMPP under complex operating conditions of TEG systems. GRNNFDO has reduced the tracking time of TEG systems by up to 50%. The statistical analysis-based study is studied such as relative error (*RE*), Success rate (*SR*), root mean square error (*RMSE*), and mean absolute error (*MAE*).

The manuscript is organized as follows: Modeling and the configuration of TEG system are explained in Section 2, Proposed GRNNFDO technology is explained in Section 3, GRNNFDO, CSA, GHO, and PSO based results are presented in Section 4, the summary of results with common discussions are presented in Section 5 and at the end, the manuscript is concluded in Section 6.

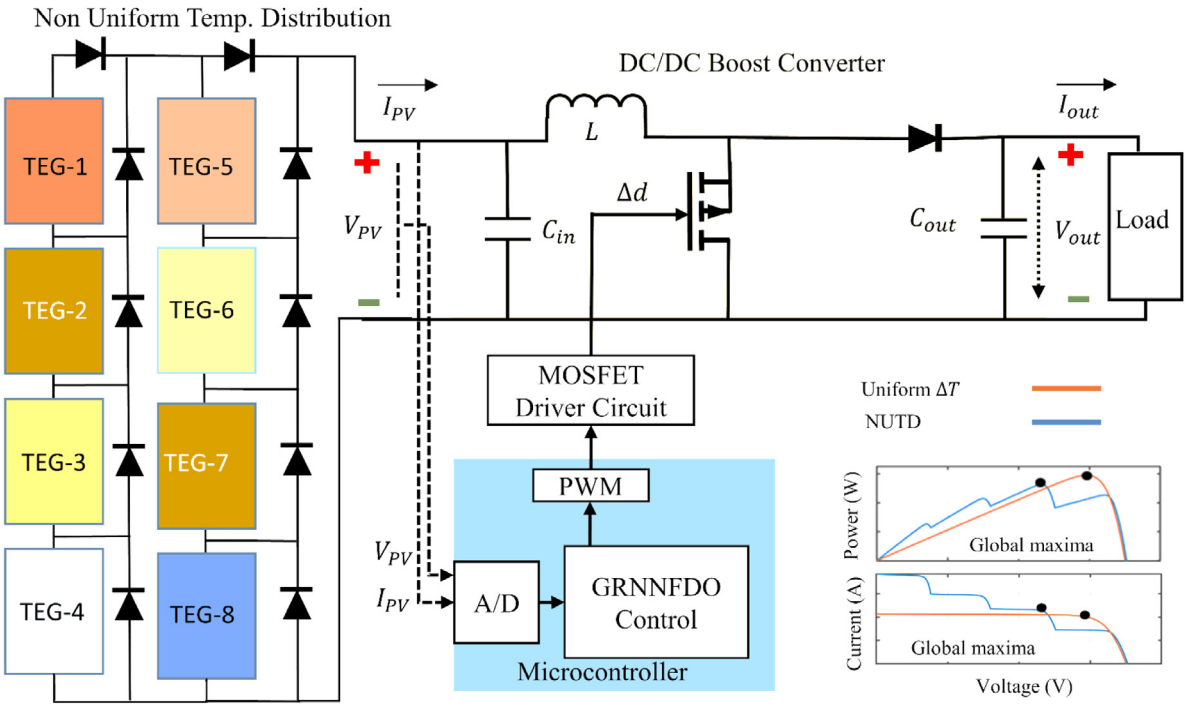


**Fig. 1.** TEG modules linked with *DC − DC Boost converter* through proposed GRNNFDO control.

## 2. Modeling of TEG system

The equivalent TEG model is shown in Fig. 1. Fig. 1 shows that the TEG module behaves as a voltage source ($Voltage_{source}$), $R_{TEG}$ is the resistance connected with TEG. Open-circuit voltage is defined as $V_{OC}$ The open-circuit voltage $V_{OC}$ can be described in Eq. (1) as.

$$V_{oc} = \alpha_{pn}\,(T_h - T_c)\,n = \alpha_{pn}\Delta T n \tag{1}$$

where $\Delta T$ is the variation of temperature on hot sides ($T_h$) and variation of temperature on the cold side defined as ($T_c$). $n$ is the total number of TEG modules, $\alpha_{pn}$ is Seebeck co-efficient.

Usually, the Seebeck effect on TEG and Thomson effect on TEG is important. The Thompson co-efficient in the TEG is defined as $\tau$ and it can be modeled as

$$\tau = T\frac{d_{\alpha pn}}{dT} \tag{2}$$

Hence, the more precise Seebeck co-efficient can be gotten with the variation in mean temperature $T$, which is stated in Eq. (3).

$$\alpha\,(T) = \alpha_o + \alpha_1 l_n\left(\frac{T}{T_o}\right) \tag{3}$$

where $\alpha_o$ is the elementary part of Seebeck coefficient. As $\alpha$ is the rate of difference of Seebeck coefficient and $T_o$ is denoted as the temperature reference. The output power of TEG can be defined as

$$P_{TEG} = \left(\alpha_{pn}\right)^2 \frac{R_1}{(R_{L+}R_{TEG})^2} \tag{4}$$

where $R_1$ and $R_{TEG}$ are the load resistance of TEG and internal resistance of TEG, $P_{TEG}$ is the power produced by TEG. TEG module electrical parameters are presented in Table 1 (see Fig. 2).

### 2.1. Configuration of TEG system

TEG systems can produce good output power for various applications. Different type of TEG module arranging has been studied in the literature. The grouping of TEG modules in series & parallel configurations can increase the output power ratings. Distributed-TEG System with multiple control units is shown in Fig. 3 & Centralized-TEG system with single control unit is presented in Fig. 4 (Zhang et al., 2020).

**Table 1**
TEG module parameters used in this study.

| Parameter | Conditions | Value |
|---|---|---|
| $P$ | $Th = 250, Tc = 50$ *@Matched Load* | 24.3 W |
| $V_{OC}$ | $Th = 250, Tc = 50$ | 10.8 V |
| $V_{LOAD}$ | $Th = 250, Tc = 50$ | 5.4 V |
| $R_{TEG}$ | $Th = 250, Tc = 50$ | 1.2 Ω |
| $I_{LOAD}$ | $Th = 250, Tc = 50$ *@Matched Load* | 4.5 A |

### 2.2. TEG system mathematical modeling under NUTD

The productivity of the industrialized Centralized-TEG system differs from the working conditions. Nowadays, every TEG module works on a dissimilar Temp. $T$ level. The mathematical equation of the TEG system is presented in Eq. (5).

$$I_i = \begin{cases} (V_{oci} - V_{Li}) & \frac{I_{sci}}{V_{oci}} = I_{sci} - \frac{V_{Li}}{R_{TEGi}} 0 < V_{Li} \le \frac{I_{sci}}{V_{oci}} \\ 0 & otherwise \end{cases} \tag{5}$$

$P_{TEGi}$ can be modeled as Eq. (6)

$$P_{TEGi} = \begin{cases} V_{Li}I_i = I_{sci}V_{Li} - \frac{I_{sci}}{R_{TEGi}} & if\ 0 < V_{Li} \le \frac{I_{sci}}{V_{oci}} \\ 0 & otherwise \end{cases} \tag{6}$$

The total power of the TEG module is

$$P_{TEGE} = \sum_{i=1}^{N} P_{TEGi} \tag{7}$$

The dissimilar temperature levels on the TEG devices will create several peaks on the PV curve of the TEG modules, as shown in Fig. 5(b). This demonstrates that under NUTD, there

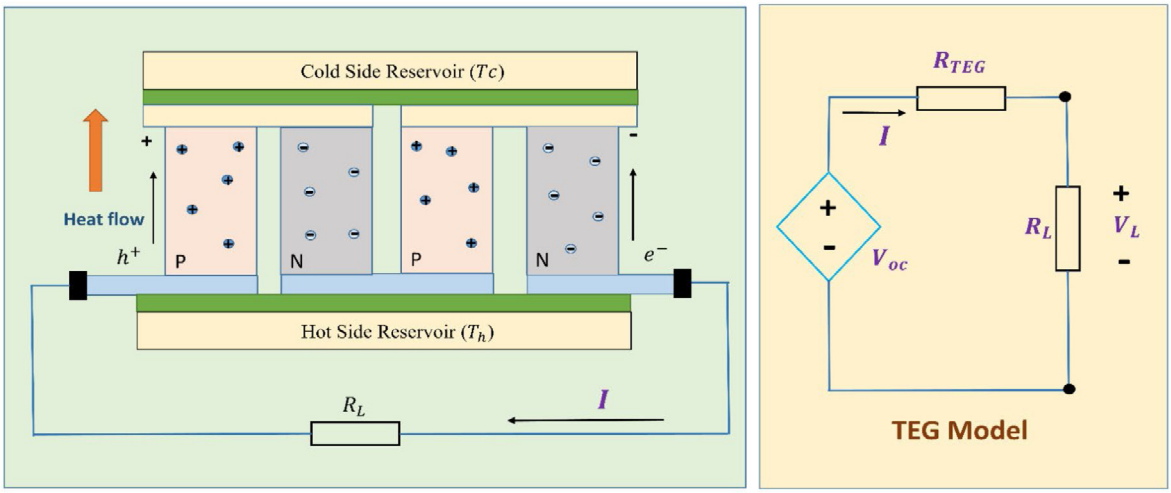


**Fig. 2.** Equivalent detailed model of TEG module.

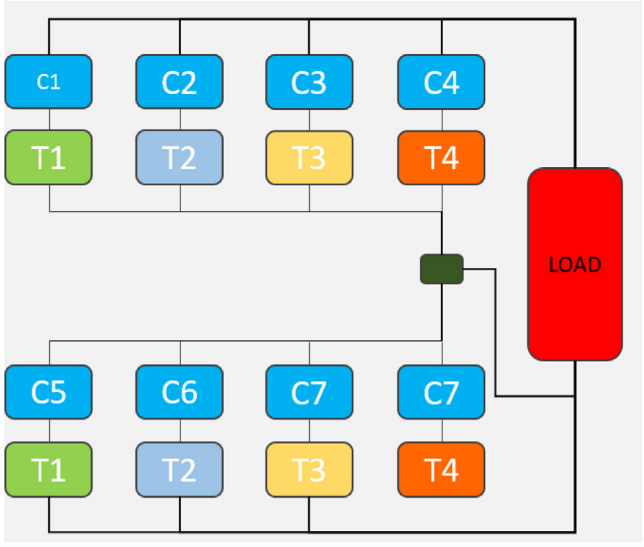


**Fig. 3.** Distributed TEG system.

is only one GMPP and several local maxima. Yet, TEG modules working under uniform temperature exhibit only one MPP, as shown in Fig. 5(a). So, under *NUTD*, a dynamic MPPT control methodology is required to efficiently trace the GMPP and extract the maximum power for the TEG modules.

## 3. Proposed technique based on GRNN with FDO

General regression neural network was first presented in Specht (1991). GRNN is very simple and needs a few samples of data to train. The benefit of using the probabilistic neural network (PNN) is that it displays good convergence and fast response for the defined function. GRNN structure is separated into four layers. A four-layer GRNN is presented in Fig. 6, GRNN primarily estimates the linear or non-linear regression for the defined input vector in terms of $X_j = [x_1, x_2, \ldots .x_n]^T$ and gives the output vector $Y_j = [y_1, y_2, \ldots .y_n]^T$.

The output $Y(x)$ is represented by

$$Y(x) = \frac{\sum_{j=1}^{n} w_j \exp\left[-\frac{K_j^2}{2\sigma^2}\right]}{\sum_{j=1}^{n} \exp\left[-\frac{K_j^2}{2\sigma^2}\right]} \tag{8}$$

$$K_j^2 = (x - x_j)^T (x - x_j) \tag{9}$$

$$Y_j = -\exp\left(\frac{(x - x_j)^T (x - x_j)}{2\sigma^2}\right) \tag{10}$$

GRNN consists of four layers, Input layer (IL), Pattern Layer (PL), Summation layer (SL) and the final Layer of GRNN is called the output layer (OL). In (8) and (9), the parameter $K_j^2$ is the distance among the predicted data of output layer and the trained data set vector. $x$ denotes to Input vector, $x_j$ is the trained vector data of the PL. PL neurons use the Gaussian function $Y_j$ in (10). The term $w_j$ is the weight of the neuron $j_{th}$ in PL linked with the SL. Arithmetic summation is defined as $S_s$ and weighted summation as $S_w$. The output vector is denoted as $Y$. The self-defined parameter of GRNN, which has to be calculated, is the spread parameter that is defined as variance $\sigma$ of the basis function. In order to automatically tune the *GRNN*, FDO is used to calculate the value of $\sigma$.

$$S_w = \sum_{j=1} w_j Y_j \tag{11}$$

$$Y = S_S / S_W \tag{12}$$

### 3.1. Fitness dependent algorithm for TEG system

Fitness dependent optimization (FDO) is a recent optimization technique in the swarm intelligence (SI) category (Abdullah and Ahmed, 2019). It is based upon the swarming behavior of bees during a reproductive process in the search for new hives.

The major contributions of FDO based MPPT control are

1. Implementation of novel bee swarm behavior for MPPT problem of PV systems undertaking PS problem by fitness function used for generation suitable weights that help the algorithms that algorithm is exploration as well as exploitation phase. Resultantly faster convergence towards Gm is achieved with the maximum exploration of search space.

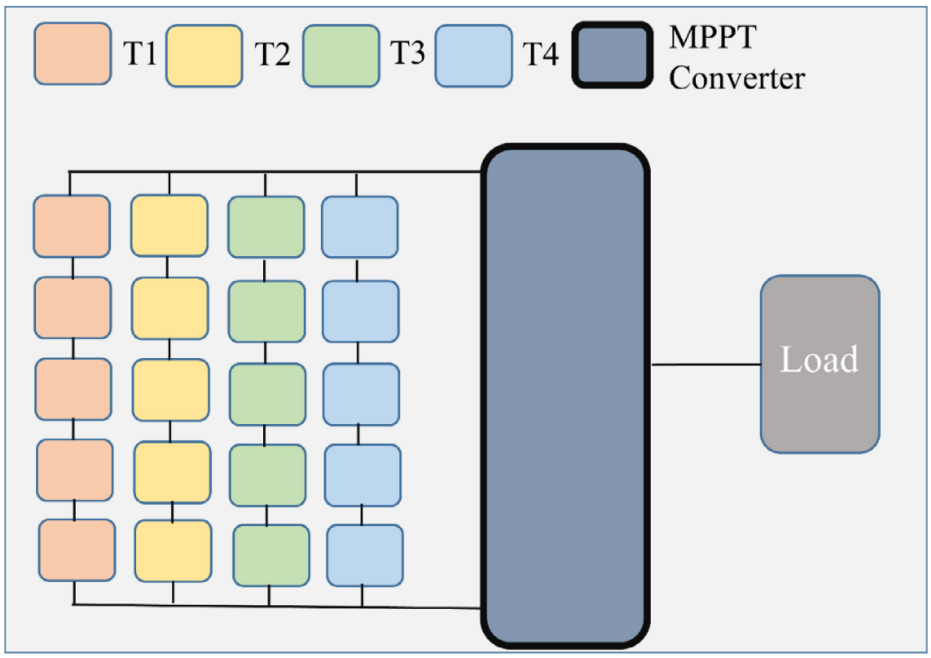


**Fig. 4.** Centralized TEG system.

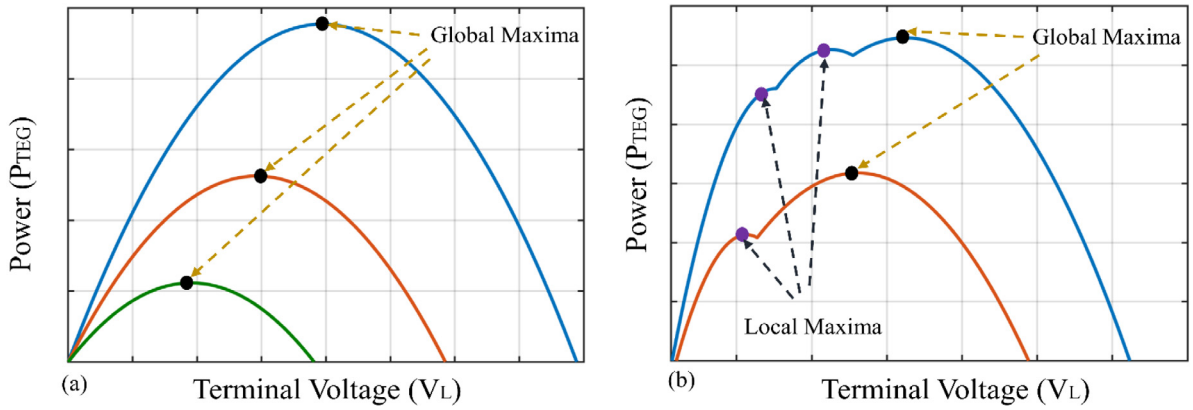


**Fig. 5.** (a) TEG under uniform temperature (PV curve) (b) TEG under NUTD (PV curve).

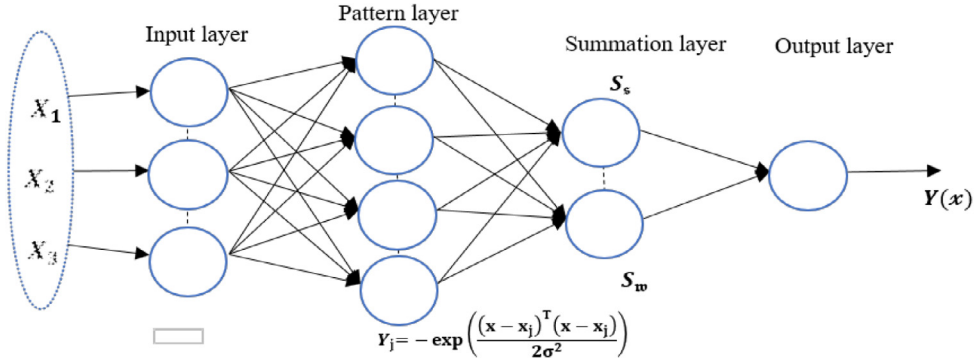


**Fig. 6.** Four layer GRNN.

2. A unique feature of FDO is the utilization of the pace variable for use in the next iterations, which incorporates learning and intelligence in the consecutive iterations
3. It is a swarm-based intelligence technique for position updating mechanism using only two variables and outperforms the competing techniques
4. The FDO successfully undertakes uni-model, multi-model, and composite functions

*3.1.1. FDO*

The FDO is a swarm intelligence-based optimizer. The FDO mimics the behavior of reproducing honeybees in search of new

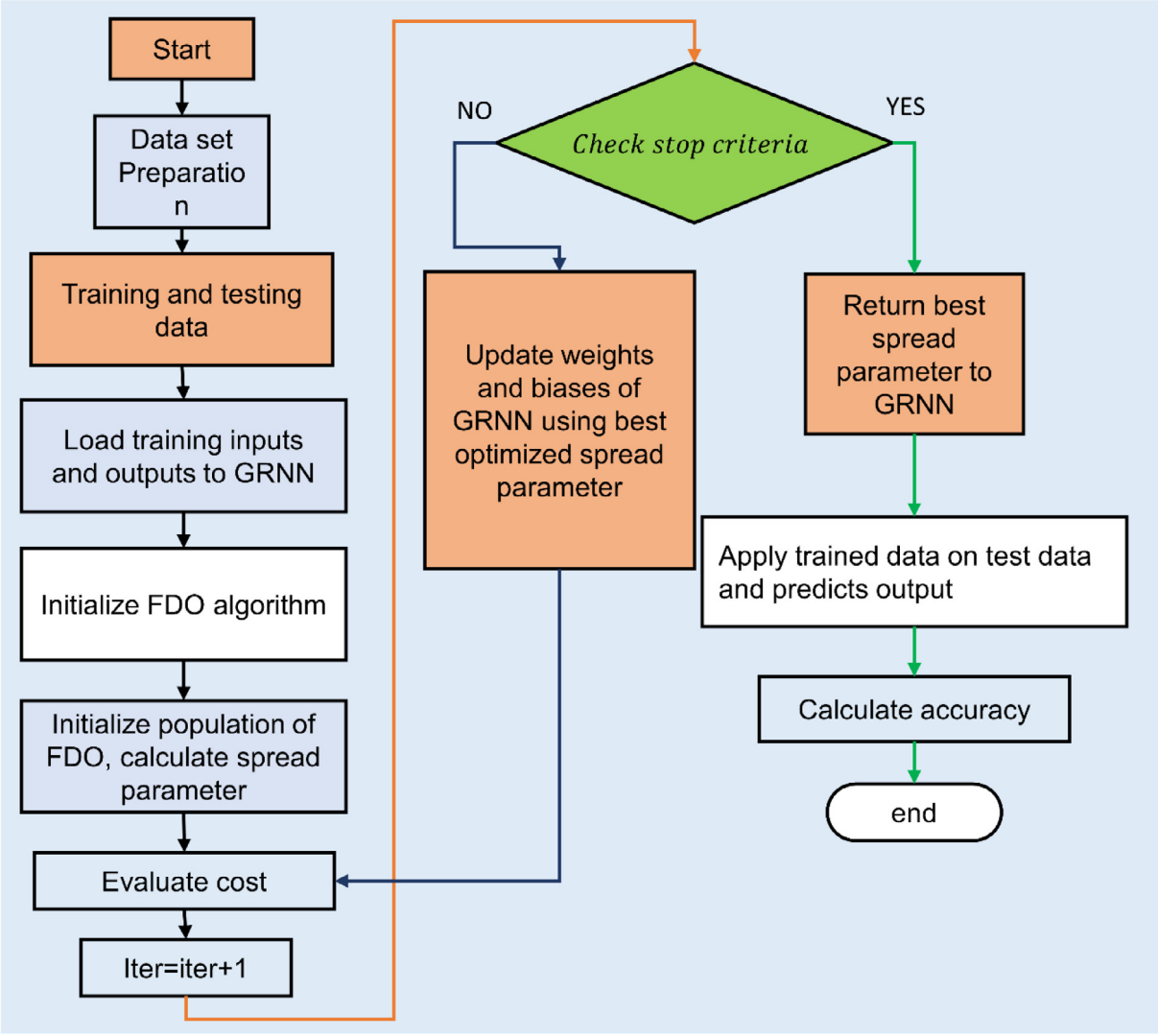


**Fig. 7.** The flowchart of GRNNFDO based MPPT control.

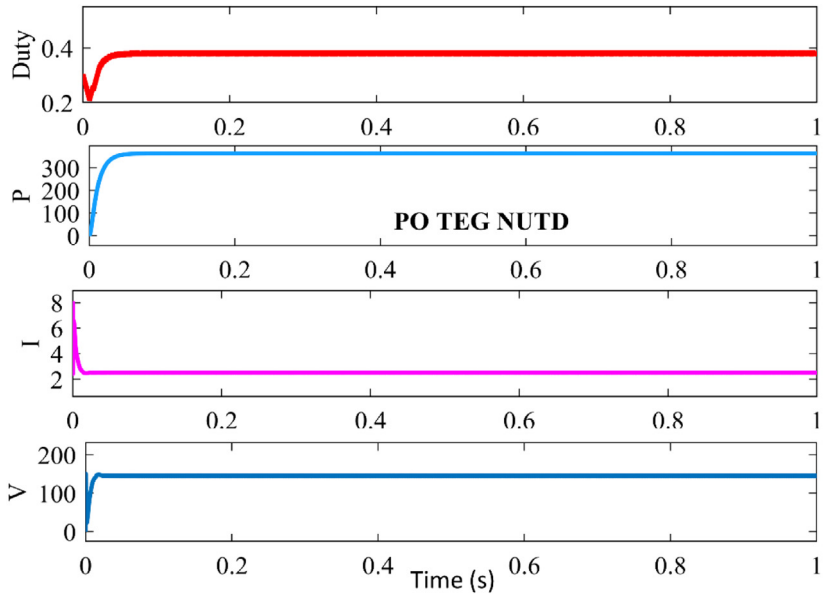


**Fig. 8.** PO tracking of GMPP under NUTD.

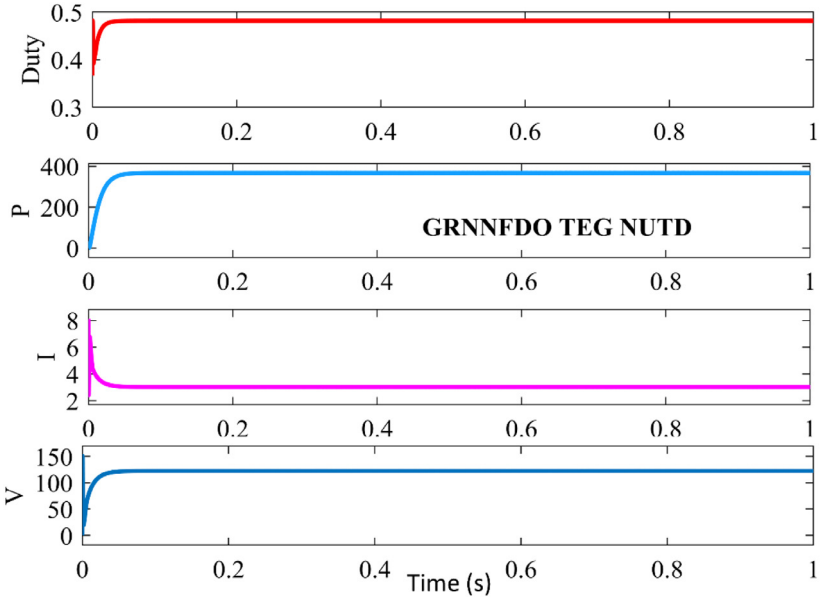


**Fig. 9.** GRNN tracking of GMPP under NUTD.

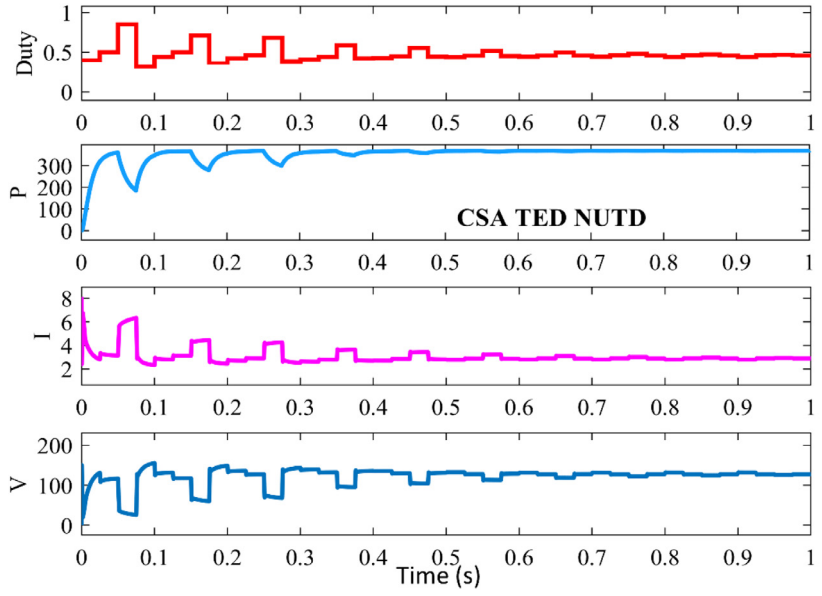


**Fig. 10.** CSA tracking of GMPP under NUTD.

locations for hives. The social interaction and lifecycle of honeybees are unique and bees are social workers. The swarm is classified into three hierarchies: queen, social workers and scouts. The queen bee is responsible for the survival of the colony. Workers provide food and protection and scout bees provide random information and search the area for food. Preferred targets are communicated to the worker bees and a collective decision-making process is invoked. The information is conveyed by specific scout bee bees and interpreted by onlookers through wiggle dance. The decision is made when the majority of information reinforces the scout search results.

### 3.1.2. Mathematical model of FDO

The FDO has a simple mathematical model which is developed to replicate the behavior of honeybees during reproduction. The main part is played by the scout bees' searching mechanism in search of a suitable hive location. The scout bees present a potential solution. The selection of the scout bee is made based on fitness. The fitness function is potentially maximized or minimized. The first step in FDO is to randomly initialize the artificial scout population in the search space for $n$ number of searching agents in $j$th dimensional search space as in Eq. (13)

$$X_i^j = X_1, X_2, X_3, \ldots, X_n * rand \tag{13}$$

where $X_i$ $(1, 2, 3, \ldots, n)$ ; each position of scout provides a potential solution. The fitness of each solution is calculated and sorted. In each iteration, the searching member updates the location using the initial location and pace as given in Eq. (13). If a better solution is attained, the weaker solutions are abandoned. If the current solution does not improvise, the previous fitness solution is maintained. This helps to avoid large fluctuations in the initial phase.

In nature, the search is done randomly. To mathematically mimic the random conduct of moving FDO agents, random walk

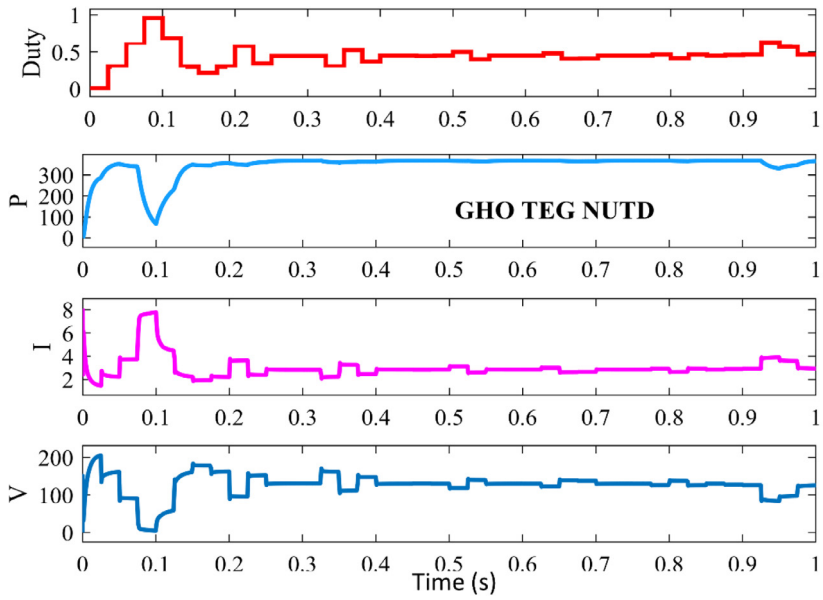


**Fig. 11.** GHO tracking of GMPP under NUTD.

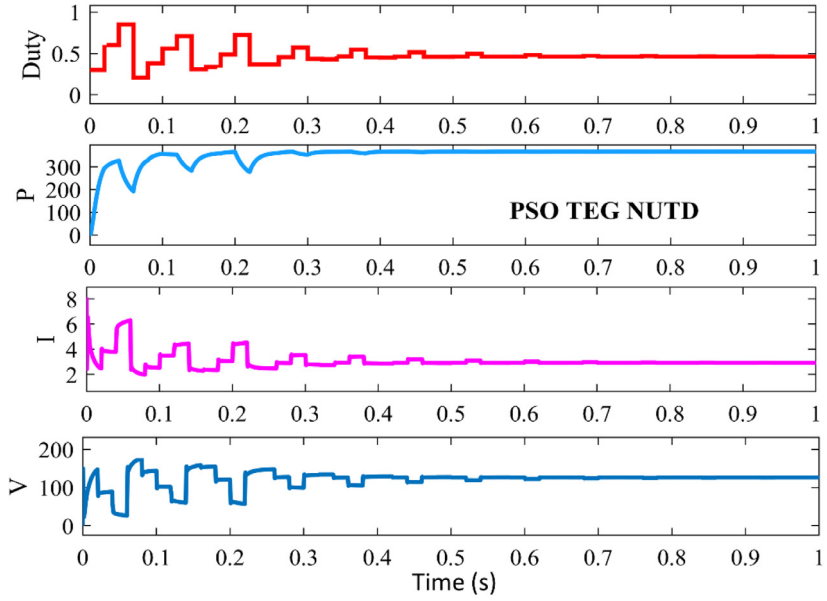


**Fig. 12.** PSO tracking of GMPP under NUTD.

and fitness weight mechanisms are incorporated into the model. The movement of FDO particles is done by adding a pace to its current position. The movement in the search space is governed by Eq. (14)

$$X^{j}_{i,(l+1)} = X_{i,l} + pace \tag{14}$$

where $l$ is the current iteration, $X^{j}_{i,(l+1)}$ is the updated position in the next iteration $(l+1)$ for $i$th particle in $j$th dimension and $pace$ is the random number generated based on fitness weights $(fw)$ of the random walk mechanism in a random direction. The $fw$ is calculated by Eq. (15)

$$fw = \left| \frac{x^{*}_{i,l}\, fitness}{x_{i,l}\, fitness} \right| * wf \tag{15}$$

where $x^{*}_{i,l}$ is the fittest particle, $x_{i,l}$ is the fitness of the $i$th particle in $l$th iteration, $wf$ is the weight factor and its value is 1 or 0. If $wf = 1$ indicates the high rate of convergence but convergence time becomes elongated. To supplement the slower convergence $wf$ is kept 0. The Eq. (30) is not affected by $wf$ and hence can be deserted. Still, in some cases, the fitness value is dependent upon the problem. In some cases, i.e., if the current values are the GM, the $fw = 1$ or global and current solutions become equal. Therefore these values are kept within 0–1. The $wf$ factor controls the $fw$. In case when $fw = 0$ and $x^{*}_{i,l}\ fitness = 0$, the division by zero should be avoided for $x_{i,l}\ fitness = 0$. The rules defined in Eqs. (16)–(17)(b) are utilized to avoid division by zero, which affects the pace as

$$fw = 1 \ or \ fw = 0 \qquad x_{i,l}\, fitness = 0, \qquad pace = x_{i,l} \cdot r \tag{16}$$

$$fw > 0 \ and \ fw < 1 \begin{cases} r < 0, & pace = \left(x_{i,l} - x^{*}_{i,l}\right) \cdot fw - 1 \quad (a) \\ r \geq 0, & pace = \left(x_{i,l} - x^{*}_{i,l}\right) \cdot fw \quad (b) \end{cases} \tag{17}$$

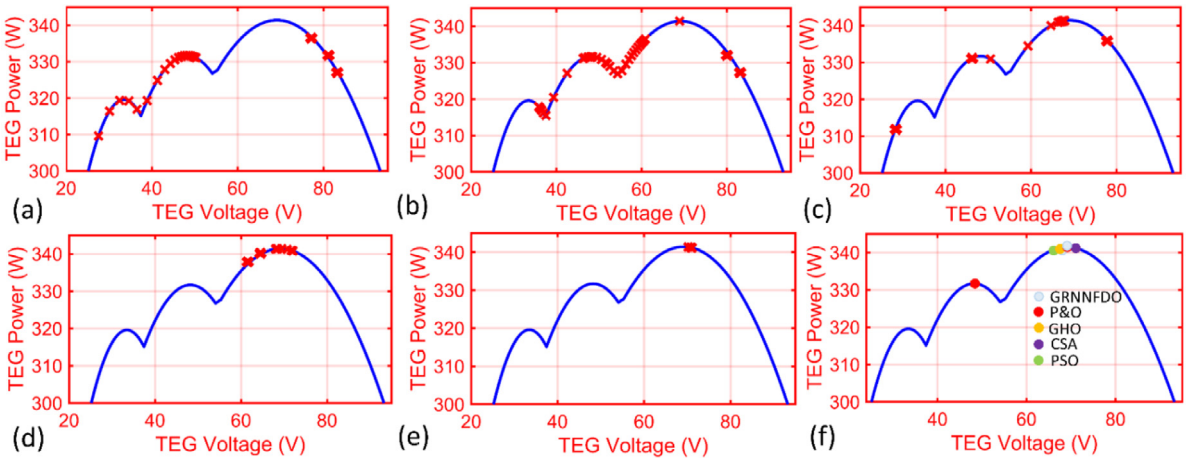


**Fig. 13.** Case study 2: GRNNFDO GMPP tracing under NUTD.

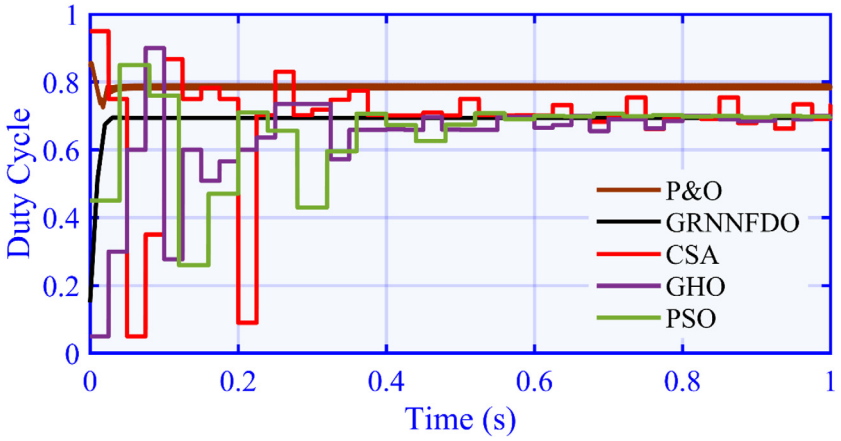


**Fig. 14.** Case study 2: Duty cycle of GRNNFDO with other control techniques.

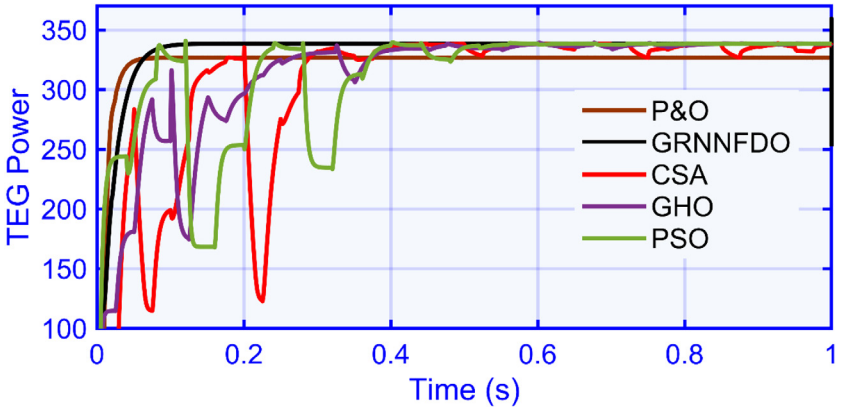


**Fig. 15.** Case study 2: Output power of GRNNFDO GRNNFDO with other control techniques.

where $r$ is a random number with a range of $[-1,1]$. The random walk is implemented using the Levy flight function for two reasons. The first is that it has stable movement because of the better distribution function and the second is that the sigma function is realizable and fine-tuning is possible (Yang, 2010). The flowchart of GRNNFDO based MPPT control is presented in Fig. 7.

## 4. Results and case studies discussion

The results and statistical indices of the GRNNFDO are evaluated and compared against the recently established control techniques such as PSO (Renaudineau et al., 2014; Ishaque et al., 2012; Priyadarshi et al., 2020), CSA (Mirza et al., 2019), P&O, and GHO. Different experimental case studies have been done,

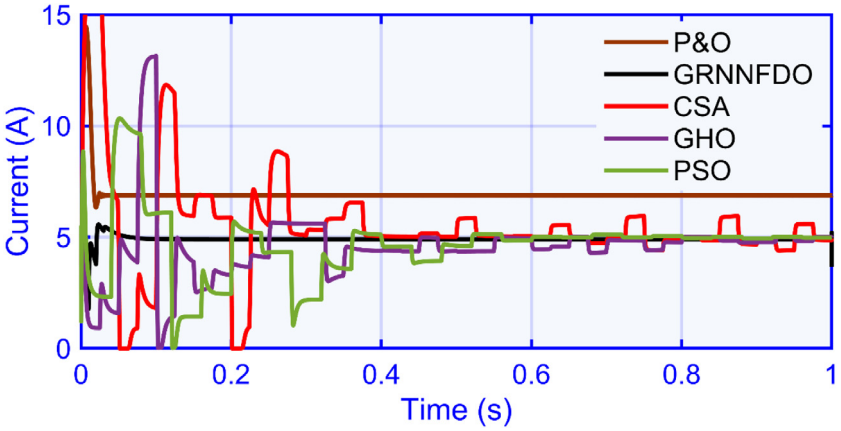


**Fig. 16.** Case study 2: Current of GRNNFDO GRNNFDO with other control techniques.

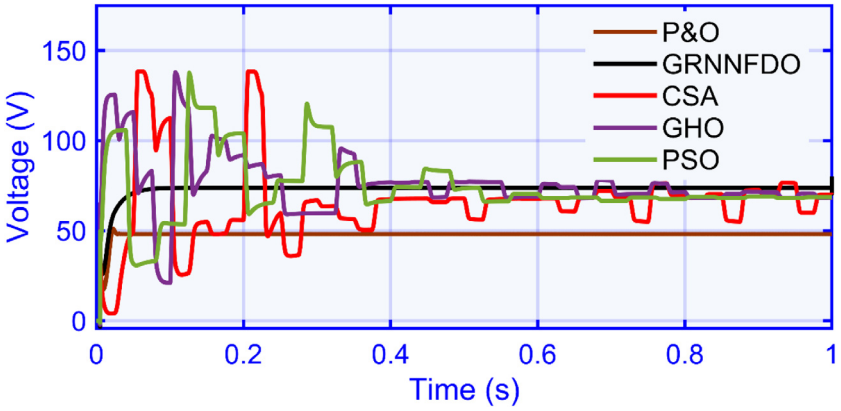


**Fig. 17.** Case study 2: Voltage of GRNNFDO GRNNFDO with other control techniques.

including NUTD case1, NUTD case 2, varying temperature case 3, and experimental study of TEG emulator case 4.

### 4.1. Case study 1: Non-uniform temperature distribution (NUTD)

Case 1 deals with the NUTD problem. In this case, there is an existence of multiple Local minimum power point (LMPP) and one true GMPP at 367.6 W. The GMPP exists closely to two LMPPs and in this condition, it is not an easy task to track the GMPP by conventional MPPT control techniques such as *P&O*, HCA and ICA. These techniques can trap LMPP and result in significant power loss as happened in our studied P&O case shown in Fig. 8. In the given scenario, the LMPP exists at ∼337 W and P&O traps at LMPP. Under GRNNFDO and CSA, the magnitude of the duty cycle curves is presented in Fig. 9. The duty cycle tracking behavior describes the optimum performance of GRNNFDO. Particularly the GMPP is located in 0.12 s, which is much faster compared to GHO, CSA, and PSO. Max. power traced by GRNNFDO is 367.6 W, followed by GHO 366.3 W, PSO 365.2 W, CSA 365.1 W, and P&O 337 W. The *mean average power* of GRNNFDO is 360 W, GHO is 355.5 W, PSO is 350.9 W, CSA is 345.4 W, and P&O is 334.4 W, respectively.

GRNNFDO tracks the GMPP within 130 ms and further takes only 10–20 ms to settle at GMPP while GHO takes 320 ms, CSA takes 460 ms, and PSO takes 480 ms, to track GM and additionally 250 ms, 380 ms, and 450 ms to settle at GMPP, respectively. GRNNFDO has the minimum tracking and settling time. P&O has a very good tracking speed and easy execution, but its inability to locate GMPP will lead to serious power loss. Although PSO takes a relatively long time, as shown in the power tracking curve in Fig. 12, it still achieves a high average power, which indicates that the algorithm of updating the position in the search space using the levy flight function produces large fluctuations, resulting in more power and energy loss. Fig. 10 shows that CSA can search for more space. GHO duty cycle and power tracking are shown in Fig. 11.

### 4.2. Case study 2: Non-uniform temperature distribution

Case 2 is closely associated with peaks occasion of NUTD. In this case, the GMPP magnitude is 338.6 W. This case also defines the problem of closely connected max. power points where GMPP is fairly near to the next LMPP. This case study is done to investigate swarm-based technologies and the performance of the dynamic PV curve of the TEG system. GRNNFDO tracking patterns on the $P-V$ cures are illustrated in Fig. 13. The duty cycle of GRNNFDO and output power curves of GRNNFDO are compared in Figs. 14 and 15, correspondingly. The tracking time of GRNNFDO is 120 ms, CSA is 337 ms, PSO is 386 ms, and GHO is 320 ms. The settling time of GRNNFDO is 10–20 ms, GHO is 120 ms, CSA is 180 ms, and PSO is 185 ms. The max. power traced by GRNNFDO is 338.6 W trailed by GHO 336.5 W, CSA 334.2 W, PSO 333.7 W, and P&O 320.8 W.

The *average power* of P&O is not very good as in this case P&O is stuck at the LMPP, P&O also displays the fluctuations around the traced LMPP. As output curves show in Figs. 16 and 17, P&O suffers from the LMPP trap. The general performance of the tested MPPT methodologies can be graded as *GRNNFDO* > *GHO* > *CSA* > *PSO* > *P&O*.

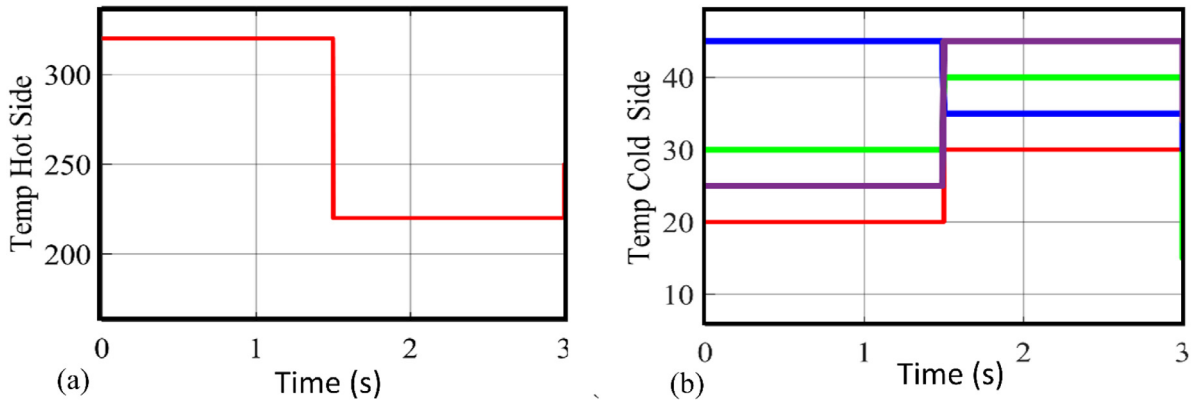


**Fig. 18.** Case study 3: Temperature variation of TEG system (a) *Cold side*; (b) *Hot side*.

### 4.3. Case 3: Varying temperature

This test inputs a sequence of temperature patterns, as mentioned in Fig. 18, to confirm the MPPT control action of GRNNFDO. And as illustrated in Fig. 18(a), the $T$ inputs of the cold side of the TEG are the non-identical curves for the whole strings. The hot side of the TEG is exposed to the working environment and is tested in the $T$ levels of 225 C and 325 C.

The time taken for tracking the GMPP by GRNNFDO, CSA, GHO, PSO, and P&O is 120 ms, 490 ms, 430 ms, 560 ms, and 120 ms and it further takes 10–20 ms, 140 ms, 120 ms, 230 s, 20–30 ms

To Stabilize without fluctuation. As shown in Fig. 19, PSO shows the maximum fluctuation. This is because the PSO location is updated using the information shared by the individual best vector and global best vector. In every cycle, the weights and random numbers used in the velocity equation are updated. Randomness affects the proportion of control parameters. For GHO, the initial exploration phase is invalid. GHO uses a comfort zone where exploration and development are balanced. However, because MPP is closely related, the comfort zone is tough to keep. The TT of GRNNFDO is 63.7% faster compared to PSO, followed by CSA 54%, and GHO at 50.8%. As depicted in Fig. 20, the power traced by GRNNFDO, GHO, CSA, PSO, and P&O is 1628.6 W, 1625.4 W, 1626.5 W, 1626.0 W, *and* 1625 W with an average efficiency of 99.99%, 99.80%, 99.36%, 99.52%, 99.15%, respectively. The average power in the complete interval of GRNNFDO is 918.4 W, GHO is 902.7 W, CSA is 887.5 W, PSO is 884 W, and P&O 883.6 W. Firstly the flaw of PSO caused by the weighted vector of velocity is exposed and CSA is unable to track GM in CPS. Secondly, techniques such as GHO can locate the GMPP but have low average power. The higher average power is The overall performance sequence in case 4 is *GRNNFDO* > *GHO* > *CSA* > *PSO* > *P&O*. Figs. 21 & 22 show stable output voltage and current.

### 4.4. Case 4: Varying load condition

In this case study, the proposed GENNFDO is used with the PI controller, as the behavior of the load and usage of a working environment can vary suddenly. If the reference voltage (Vref) is not tunned instantly, according to the maximum power transmission theorem, the mismatch between the boost converter and the update load will lead to a serious loss of available power. This problem has caused a major loss of power in grid-connected operations. The conventional technique of PID tunning by using Ziegler–Nichols(ZG) can yield fluctuation at the transition point of load. The current research using a direct current sweep study shows that for the TEG module, the *Voltage* oscillation may rise to

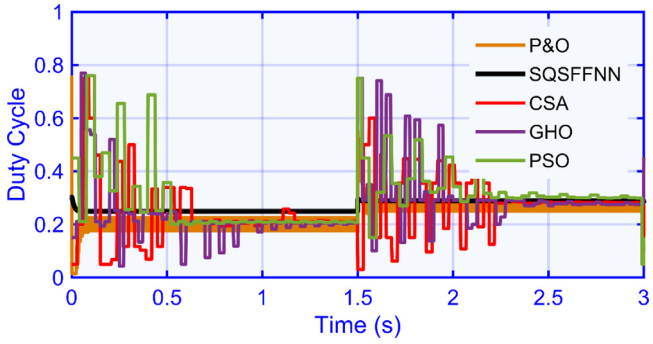


**Fig. 19.** Case 3: Step change temperature condition duty cycle curve of GRNNFDO.

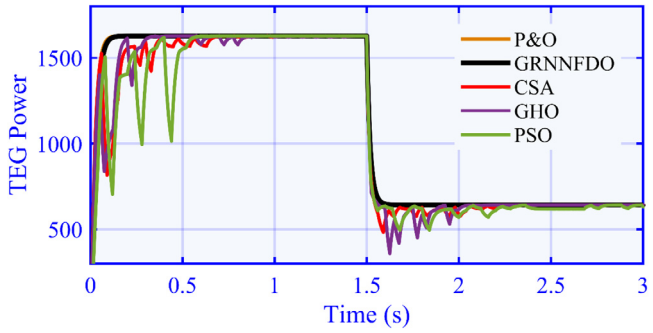


**Fig. 20.** Case study 3: Step change temperature condition power curve of GRNNFDO.

2.501 V, reaching 9.5% of the peak rating. However, the proposed GRNNFDO with PI controller can successfully eradicate the voltage oscillation and progresses the protection of load appliances. The load varies from 11 to 15 Ω to 6 Ω , then 25 Ω for a constant $T_{hot}$ and $T_{cold}$. Calculate every half second. The reference voltage calculation is only affected by the change of load impedance. The performance of the proposed GRNNFDO will be measured when the load changes periodically. The Fig. 23. Displays the transient actions of GRNNFDO based PID MPPT controller, It displays that there are limited fluctuations, and comparatively low time is required to trace the set value of *voltage* comparative to the ZG technique based PID as illustrated in Fig. 24. Moreover, results demonstrate that the settling time of GRNNFDO with PID controller for the varying load is 60% lower than ZG method.

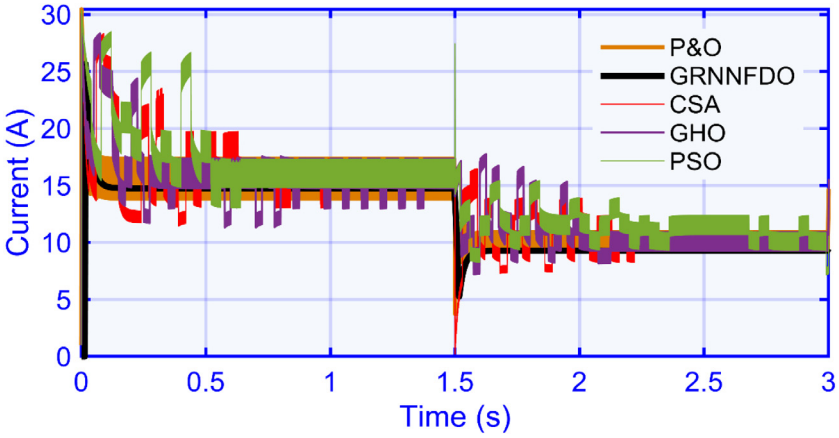


**Fig. 21.** Case study 3: Step change temperature condition current curve of GRNNFDO.

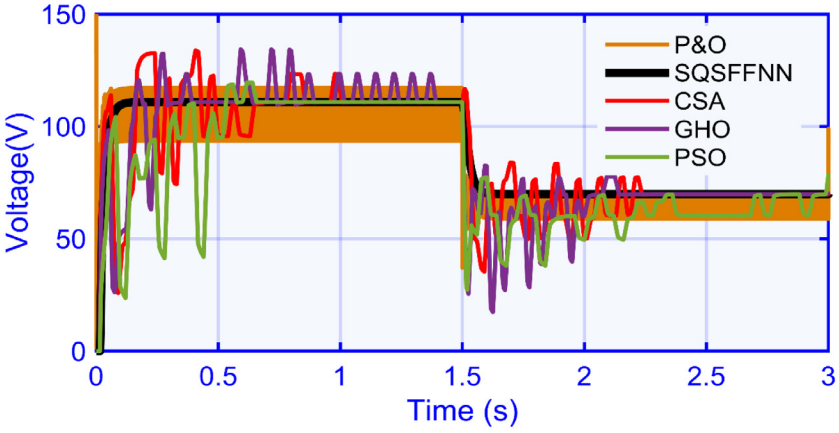


**Fig. 22.** Case study 3: Step change temperature condition voltage curve of GRNNFDO.

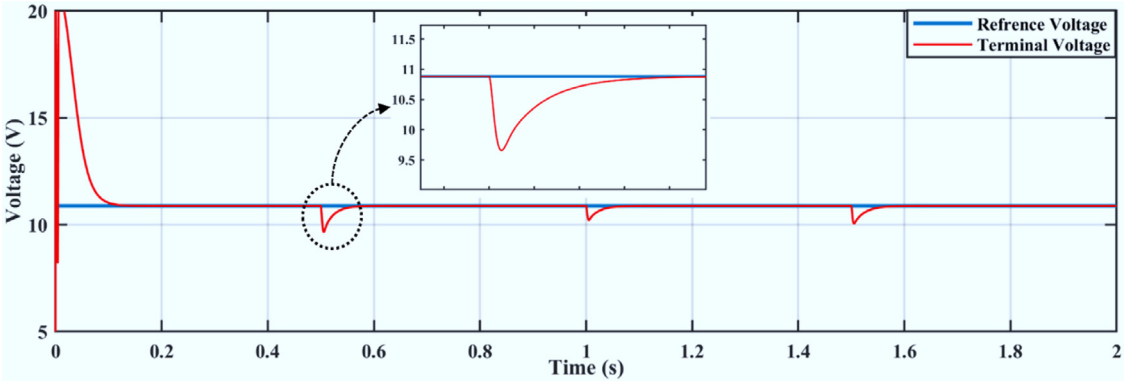


**Fig. 23.** Varying load output of GRNNFDO trained PID controller.

### 4.5. Case 5: Experimental study of TEG emulator

To authenticate the MPPT control implementation for TEG systems, a cost-effective TEG practical simulator is utilized. As explained in Section 2, TEG output is very dependent on the temperature values and it acts as a $V_{source}$ whose *Voc* changes with the surrounding temperature. Therefore, the DC supply with $V_{high}$ and $R_L$ in series simulates the effect of the TEG module. The power ratings of the emulator are set according to the experiment demands. Fig. 25 shows the connection of components with the $DC-DC$ *boost converter*, $Current_{sensor}$, $Voltage_{sensor}$, $\mu controller$ and $Load(R_L)$. The experimental hardware system of the TEG emulator is shown in Fig. 26. Table 2 labels the components which are used in the implementation of the TEG emulator system.

Fig. 27 displays the power traced by CSA under changing temperature conditions, which authenticates that CSA took up to 400 ms to trace and settle down at GMPP. After attaining the GMPP, little fluctuations can be observed. CSA settle down at less power, causing significant output power loss and reducing the overall efficiency of MPPT control. Whereas in comparison with CSA, GRNNFDO traces and settles down at GMPP within 200 ms, as displayed in Fig. 27. In comparison with CSA, GRNNFDO shows

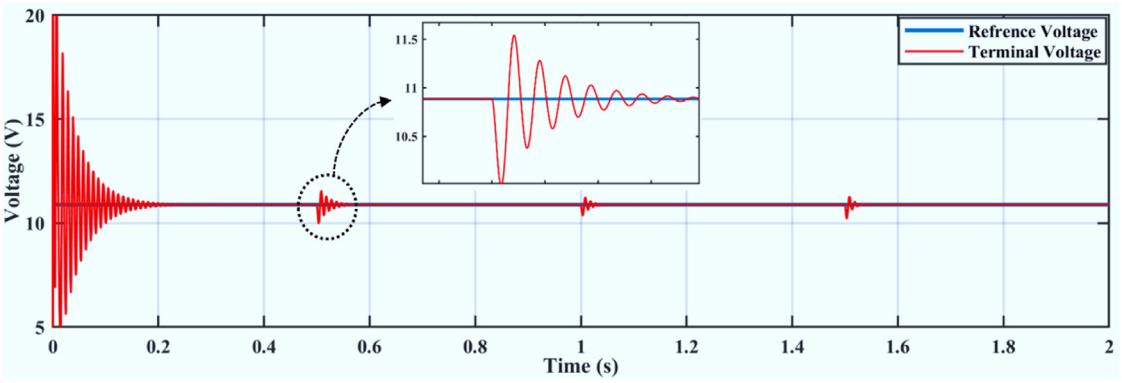


**Fig. 24.** Varying load output of ZN trained PID controller.

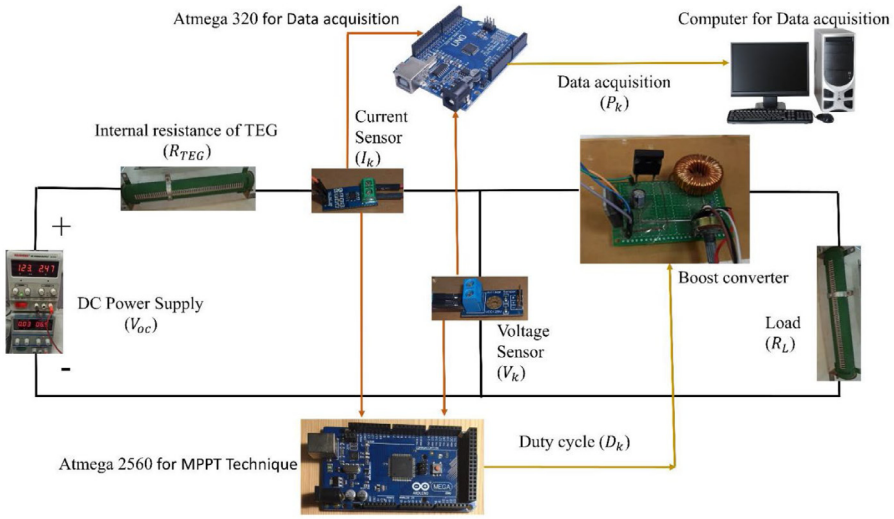


**Fig. 25.** Implementation of TEG system control on a low-priced TEG-emulator.

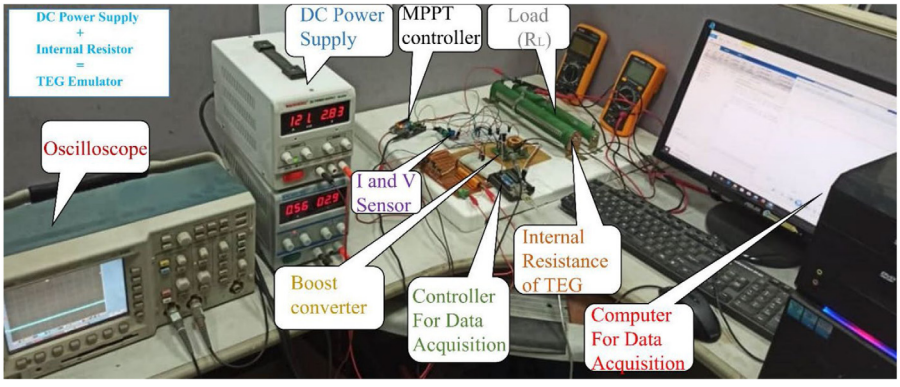


**Fig. 26.** Experimental setup for TEG system.

a very quick tracing because of the stable duty cycle response and takes less than 200 ms to track and settle down at GMPP.

## 5. Common results and discussion

This section summarizes the common findings of all case studies.

### 5.1. Settling time and tracking time

The tracking time (TT) is the time taken by the MPPT controller to locate GM and the settling time is the time taken by its searching agents in search space to converge on GMPP without further oscillations. Minimum TT and ST are preferred within the least number of iterations. Tracking time and settling time are

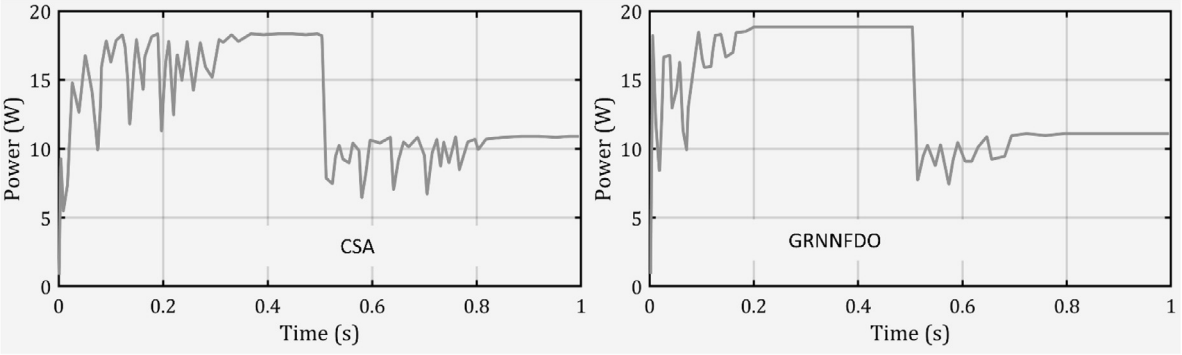


**Fig. 27.** Experiment results showing GRNNFDO and CSA max. power point tracking.

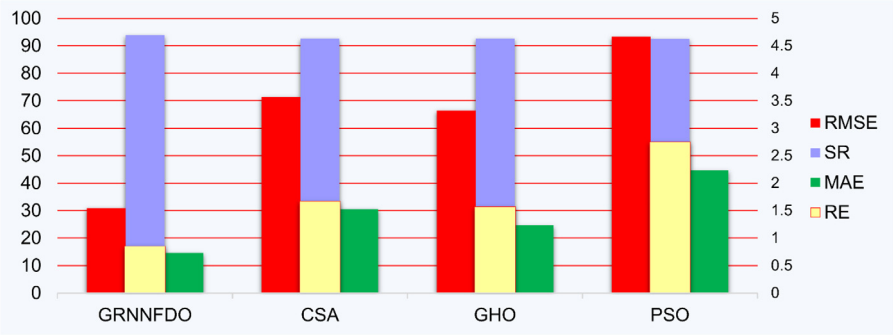


**Fig. 28.** GRNNFDO *RE*, *RMSE*, *SR*, and *MAE*.

**Table 2**
Specifications of components.

| Components | Values |
|---|---|
| Inductor, ($L$) | 1 mH |
| Input capacitor ($C_{in}$) | 100 μF |
| Output capacitor ($C_{out}$) | 1000 μF |
| MOSFET | *IRF*730 |
| Switching frequency, ($f$) | 61 kHz |
| Load, ($RL$) | 5 Ω |
| $V_{sensor}$ | *B*25 |
| $C_{sensor}$ | $ACS-172$ |
| Micro-controller | *ATmega*2560 |

two important qualitative measures. Minimum time constraints are desired from an efficient MPPT controller. The best ST and TT are achieved by GRNN FDO followed by GHO, CSA, PSO and P&O. on average proposed techniques give a 10%–20% enhancement.

### 5.2. Power tracking efficiency

The *maximum power* efficiency and *mean power* efficiencies are studied. In both indices, proposed techniques outperform opposing technologies. The NUTD cases highlight the drawbacks of PSO and CSA in power tracing efficiencies. The P&O performance remains between 60 and 80%.

### 5.3. Oscillations and fluctuations

Classical techniques have a major issue of oscillations in voltage transients around MPP. Similarly, fluctuations are observed in swarm-based technologies that utilize Levy functions or Brownian motion functions to break LM traps. These oscillations are undesirable. Proposed techniques successfully eliminate these from power and voltage transient. The ripples remain $\leq 1$ W in all cases.

### 5.4. Statistical analysis of the GRNNFDO

Here the statistical analysis of the proposed GRNNFDO techniques is made. The sensitivity of the technologies is measured by relative error (RE) Eq. (18), Success rate (SR), mean absolute error (MAE) Eq. (19) and root mean square error (RMSE) in Eq. (20) as:

$$RE = \frac{\sum_{i=1}^{n}\left(P_{pvi} - P_{pv}\right)}{P_{pv}} * 100\% \tag{18}$$

$$MAE = \frac{\sum_{i=1}^{n}\left(P_{pvi} - P_{pv}\right)}{n} \tag{19}$$

$$RMSE = \sqrt{\frac{\sum_{i=1}^{n}\left(P_{pvi} - P_{pv}\right)^2}{n}} \tag{20}$$

where $P_{pvi}$ is the output power in the $i$th run, $P_{pv}$ is the max. the possible output power of the TEG system, $n$ is the total number of runs. In addition to the measures in Eqs. (17)(b)–(20), median, means and standard deviation, and success rate (SR) are considered. The proposed technique achieves smaller RE and MAE than PSO, CSA, PSO and P&O. Fig. 28 provides the statistical analysis graphically.

## 6. Conclusion

In this work, a novel Machine learning-based control technology is proposed for the centralized TEG system under varying operating conditions. The GRNNFDO is implemented to work proficiently under non-static conditions and NUTD conditions. GRNNFDO results are compared with other MPPT technologies such as CSA, PandO, PSO, and GHO. GRNNFDO attains the finest results, tracking time of GRNNFDO is lowest, the proposed method tracks global maxima with a very good efficiency measured as >99%. GRNNFDO takes up to 110.1 ms to trace the true GMPP. GRNNFDO

oscillations around global maxima are very low in comparison with GHO, PandO, and PSO based MPPT technologies. GRNNFDO produces 8.3% more output under NUTD comparatively. It is also concluded that GRNN optimized spread parameter value is very important for efficiently tracing GMPP under various operating conditions. In the future, the more complex behavior of TEG systems will be studied and concentrated PV-TEG, Hybrid PV-TEG systems will be considered for the optimum usage of solar energy.

## CRediT authorship contribution statement

**Adeel Feroz Mirza:** Data curation, Methodology, Software, Writing, Reviewing. **Syed Kamran Haider:** Data curation, Methodology, Software, Writing, Reviewing. **Abbas Ahmed:** Conceptualization, Validation, Writing – review & editing. **Ateeq Ur Rehman:** Conceptualization, Validation, Writing – review & editing. **Muhammad Shafiq:** Conceptualization, Supervision, Writing – review & editing. **Mohit Bajaj:** Supervision, Writing – review & editing. **Hossam M. Zawbaa:** Resources, Writing – review & editing. **Pawel Szczepankowski:** Resources, Writing – review & editing. **Salah Kamel:** Resources, Writing – review & editing.

## Declaration of competing interest

The authors declare that they have no known competing financial interests or personal relationships that could have appeared to influence the work reported in this paper.

## Acknowledgments

The author (Hossam M. Zawbaa) thanks to the European Union's Horizon 2020 research and Enterprise Ireland for their support under the Marie Skłodowska-Curie grant agreement No. 847402. This work is also supported by the LINTE^2 Laboratory, Gdansk University of Technology, Poland. The authors thank the support of the National Research and Development Agency of Chile (ANID), ANID/Fondap/15110019.

## References

Abdullah, J.M., Ahmed, T., 2019. Fitness dependent optimizer: inspired by the bee swarming reproductive process. IEEE Access 7, 43473–43486.
Ahmed, J., Salam, Z., 2014. A Maximum Power Point Tracking (MPPT) for PV system using cuckoo search with partial shading capability. Appl. Energy 119, 118–130.
Ahmed, J., Salam, Z., 2018. An enhanced adaptive P & O MPPT for fast and efficient tracking under varying environmental conditions. IEEE Trans. Sustain. Energy 9 (3), 1487–1496.
Ali, A.I.M., Mohamed, H.R.A., 2022. Improved P & O MPPT algorithm with efficient open-circuit voltage estimation for two-stage grid-integrated PV system under realistic solar radiation. Int. J. Electr. Power Energy Syst. 137, 107805.
Ali, M.N., et al., 2021. Promising MPPT methods combining metaheuristic, fuzzy-logic and ANN techniques for grid-connected photovoltaic. Sensors 21 (4), 1244.
Darcy Gnana Jegha, A., et al., 2020. A high gain dc-dc converter with grey wolf optimizer based MPPT algorithm for PV fed BLDC motor drive. Appl. Sci. 10 (8), 2797.
Fathy, A., 2020. Butterfly optimization algorithm based methodology for enhancing the shaded photovoltaic array extracted power via reconfiguration process. Energy Convers. Manage. 220, 113115.
Garmejani, H.A., Hossainpour, S., 2021. Single and multi-objective optimization of a TEG system for optimum power, cost and second law efficiency using genetic algorithm. Energy Convers. Manage. 228, 113658.
Huang, C., et al., 2017. A prediction model-guided jaya algorithm for the PV system maximum power point tracking. IEEE Trans. Sustain. Energy 9 (1), 45–55.
Ishaque, K., et al., 2012. An improved particle swarm optimization (PSO)–based MPPT for PV with reduced steady-state oscillation. IEEE Trans. Power Electron. 27 (8), 3627–3638.
Kalyani, C.V., Kumar, M.S., Nagaraju, T., 2020. TEG cascaded solar PV system with enhanced efficiency by using the PSO MPPT boost converter. Int. J. Res. Eng. Sci. Manage. 3 (11), 105–110.
Khan, N.M., et al., 2022. Energy harvesting and stability analysis of centralized TEG system under non-uniform temperature distribution. Sustain. Energy Technol. Assess. 52, 102028.
Li, H., et al., 2018. An overall distribution particle swarm optimization MPPT algorithm for photovoltaic system under partial shading. IEEE Trans. Ind. Electron. 66 (1), 265–275.
Li, F., et al., 2021. Adaptive rapid neural optimization: A data-driven approach to MPPT for centralized TEG systems. Electr. Power Syst. Res. 199, 107426.
Lyden, S., Haque, M.E., 2015. A simulated annealing global maximum power point tracking approach for PV modules under partial shading conditions. IEEE Trans. Power Electron. 31 (6), 4171–4181.
Ma, J., et al., 2013. Parameter estimation of photovoltaic models via cuckoo search. J. Appl. Math. 2013.
Mansoor, M., Mirza, A.F., Ling, Q., 2020a. Harris hawk optimization-based MPPT control for PV systems under partial shading conditions. J. Cleaner Prod. 122857.
Mansoor, M., et al., 2020b. Novel Grass Hopper optimization based MPPT of PV systems for complex partial shading conditions. Sol. Energy 198, 499–518.
Mansoor, M., et al., 2021. Maximum energy harvesting of centralized thermoelectric power generation systems with non-uniform temperature distribution based on novel equilibrium optimizer. Energy Convers. Manage. 246, 114694.
Mirza, A.F., et al., 2019. Novel MPPT techniques for photovoltaic systems under uniform irradiance and Partial shading. Sol. Energy 184, 628–648.
Mirza, A.F., et al., 2020. A Salp-Swarm Optimization based MPPT technique for harvesting maximum energy from PV systems under partial shading conditions. Energy Convers. Manage. 209, 112625.
Mirza, A.F., et al., 2021. High-efficiency hybrid PV-TEG system with intelligent control to harvest maximum energy under various non-static operating conditions. J. Cleaner Prod. 320, 128643.
Mohamed, N., Aymen, F., Alowaidi, M., Bajaj, M., Sharma, N.K., Mishra, S., Sharma, S.K., 2021. Increasing electric vehicle autonomy using a photovoltaic system controlled by particle swarm optimization. IEEE Access 9, 72040–72054. http://dx.doi.org/10.1109/ACCESS.2021.3077531.
Mohanty, S., Subudhi, B., Ray, P.K., 2015. A new MPPT design using grey wolf optimization technique for photovoltaic system under partial shading conditions. IEEE Trans. Sustain. Energy 7 (1), 181–188.
Priyadarshi, N., et al., 2019. An ant colony optimized MPPT for standalone hybrid PV-wind power system with single cuk converter. Energies 12 (1), 167.
Priyadarshi, N., et al., 2020. New CUK–SEPIC converter based photovoltaic power system with hybrid GSA–PSO algorithm employing MPPT for water pumping applications. IET Power Electron. 13 (13), 2824–2830.
Renaudineau, H., et al., 2014. A PSO-based global MPPT technique for distributed PV power generation. IEEE Trans. Ind. Electron. 62 (2), 1047–1058.
Sahri, Younes, Tamalouzt, Salah, Hamoudi, Farid, Belaid, Sofia Lalouni, Bajaj, Mohit, Alharthi, Mosleh M., Alzaidi, Mohammed S., Ghoneim, Sherif S.M., 2021. New intelligent direct power control of DFIG-based wind conversion system by using machine learning under variations of all operating and compensation modes. Energy Rep. (ISSN: 2352-4847) 7, 6394–6412. http://dx.doi.org/10.1016/j.egyr.2021.09.075.
soufyane Benyoucef, A., et al., 2015. Artificial bee colony based algorithm for maximum power point tracking (MPPT) for PV systems operating under partial shaded conditions. Appl. Soft Comput. 32, 38–48.
Specht, D.F., 1991. A general regression neural network. IEEE Trans. Neural Netw. 2 (6), 568–576.
Tariq, M.I., et al., 2021. Optimal control of centralized thermoelectric generation system under nonuniform temperature distribution using barnacles mating optimization algorithm. Electronics 10 (22), 2839.
Valera, Á., et al., 2021. Efficiency improvement of passively cooled micro-scale hybrid CPV-TEG systems at ultra-high concentration levels. Energy Convers. Manage. 244, 114521.
Yang, X.-S., 2010. Nature-Inspired Metaheuristic Algorithms. Luniver Press.
Yang, B., et al., 2019. MPPT design of centralized thermoelectric generation system using adaptive compass search under non-uniform temperature distribution condition. Energy Convers. Manage. 199, 111991.
Yedala, N., Kaisare, N.S., 2021. Modeling of thermal integration of a catalytic microcombustor with a thermoelectric for power generation applications. Energy & Fuels.
Zafar, M.H., et al., 2020. Group teaching optimization algorithm based MPPT control of PV systems under partial shading and complex partial shading. Electronics 9 (11), 1962.
Zafar, M.H., et al., 2021. A novel meta-heuristic optimization algorithm based MPPT control technique for PV systems under complex partial shading condition. Sustain. Energy Technol. Assess. 47, 101367.
Zhang, X., et al., 2020. Dynamic Surrogate Model based optimization for MPPT of centralized thermoelectric generation systems under heterogeneous temperature difference. IEEE Trans. Energy Convers. 35 (2), 966–976.
Zhao, Z., et al., 2020. A dynamic particles MPPT method for photovoltaic systems under partial shading conditions. Energy Convers. Manage. 220, 113070.